

Elimination of the Greenland Ice Sheet in a High CO₂ Climate

J. K. RIDLEY

Hadley Centre for Climate Prediction and Research, Met Office, Exeter, United Kingdom

P. HUYBRECHTS

Alfred-Wegener Institute, Bremerhaven, Germany, and Department of Geography, Free University of Brussels, Brussels, Belgium

J. M. GREGORY

Hadley Centre for Climate Prediction and Research, Met Office, Exeter, and Centre for Global Atmospheric Modelling, Department of Meteorology, University of Reading, Reading, United Kingdom

J. A. LOWE

Hadley Centre for Climate Prediction and Research, Met Office, Exeter, United Kingdom

(Manuscript received 10 November 2004, in final form 9 March 2005)

ABSTRACT

Projections of future global sea level depend on reliable estimates of changes in the size of polar ice sheets. Calculating this directly from global general circulation models (GCMs) is unreliable because the coarse resolution of 100 km or more is unable to capture narrow ablation zones, and ice dynamics is not usually taken into account in GCMs. To overcome these problems a high-resolution (20 km) dynamic ice sheet model has been coupled to the third Hadley Centre Coupled Ocean–Atmosphere GCM (HadCM3). A novel feature is the use of two-way coupling, so that climate changes in the GCM drive ice mass changes in the ice sheet model that, in turn, can alter the future climate through changes in orography, surface albedo, and freshwater input to the model ocean. At the start of the main experiment the atmospheric carbon dioxide concentration was increased to 4 times the preindustrial level and held constant for 3000 yr. By the end of this period the Greenland ice sheet is almost completely ablated and has made a direct contribution of approximately 7 m to global average sea level, causing a peak rate of sea level rise of 5 mm yr⁻¹ early in the simulation. The effect of ice sheet depletion on global and regional climate has been examined and it was found that apart from the sea level rise, the long-term effect on global climate is small. However, there are some significant regional climate changes that appear to have reduced the rate at which the ice sheet ablates.

1. Introduction

Past changes to the Greenland ice sheet have been studied using ice core measurements and suggest that Greenland has been generally stable through the last glacial cycle, but may have been substantially smaller in the last interglacial (the Eemian) when the climate was several degrees warmer than today (Letreguilly et al. 1991; Cuffey and Marshall 2000; Huybrechts 2002).

Over the full course of its existence it appears that the ice sheet has experienced a range of climate conditions.

The question as to whether the ice sheet is currently in a state of equilibrium has been addressed in a number of ways. The surface mass balance has been estimated using surface climate fields from the high-resolution European Centre for Medium-Range Weather Forecasts (ECMWF) operational analyses (1992–98), together with meteorological and glaciological models of snow accumulation and surface melt water runoff/retention (Hanna et al. 2002). An alternative method is to use a regional climate model (e.g., 50-km resolution) of the Arctic, forced at the lateral boundary by large-scale atmospheric conditions from GCMs. Es-

Corresponding author address: Dr. J. K. Ridley, Hadley Centre for Climate Prediction and Research, Met Office, FitzRoy Rd., Exeter EX1 3PB, United Kingdom.
E-mail: jeff.ridley@metoffice.gov.uk

estimates of the regional net balance of precipitation and ablation may then be made from the model simulations (Kiilsholm et al. 2003; Wild et al. 2003; Box et al. 2004). Both techniques suggest that the Greenland ice sheet is currently losing mass. These model analyses are supported with observations. Satellite passive microwave imagery (Mote 2003), provides estimates of runoff based on the spatial and temporal extent of surface melt, and airborne laser altimeter surveys (Krabill et al. 2000; Thomas et al. 2001; Paterson and Reeh 2001), indicate a thinning in the ice sheet margins (lower than 2000 m) and neutral mass balance at higher elevations. Both models and observations show a high spatial and interannual variation in accumulation and ablation rates, with a standard deviation of $\sim 10\%$.

In the future, increases in atmospheric greenhouse gas concentration are predicted to cause a rise in global mean temperatures (Cubasch et al. 2001). Furthermore, it is expected that the changes will be more pronounced in high northern latitudes than in the global mean, mainly due to the positive feedback of reduced sea ice extent and snow cover on the ice-free landmasses, and consequently reduced albedo (Cubasch et al. 2001). A potential consequence of the temperature rise is the melting of the Greenland ice sheet accompanied by a large sea level increase of approximately 7 m in the case of its entire disintegration (Church et al. 2001). There is also concern that loss of the ice sheets will lead to additional changes in global climate, for instance by changing the Atlantic Ocean thermohaline circulation through the freshening effect of the ice sheet meltwater.

The large ice sheets can take millennia to fully respond to changes in climate (Drewry and Morris 1992), which makes them difficult to simulate with complex models because of the large computational costs involved. Instead, simpler earth system models of intermediate complexity (EMICs), have been used to simulate climate over such time scales. Loutre (1995) forced the Louvain la Nueve two-dimensional model (LLN-2D) EMIC, which includes relatively simple interactive ice sheets, with an elevated atmospheric carbon dioxide concentration scenario for the next 5000 yr, producing an almost complete melting of the Greenland ice sheet by the end of the simulation.

Some greenhouse warming experiments have also been conducted using a Greenland ice sheet model driven "offline" by prescribed climate warmings or by the output from an energy-balance climate model. Greve (2000) found that the decay of the ice sheet is a smooth function of forcing temperature with $+12^\circ\text{C}$ resulting in near total disintegration in 1000 yr. Variations of $\pm 10\%$ in precipitation applied over Greenland leads to an uncertainty of 20% of its current mass on the

amount of ice sheet remaining after 1000 yr. Ice dynamics in these models have the effect that surface slopes at the margin are steepened in response to increased balance gradients (Huybrechts and de Wolde 1999). These can only be matched by larger ice fluxes across the equilibrium line and thus induce an increased transfer of ice mass into the melting zone, which leads to a thickening. This causes a higher surface level of the ablation zone, and consequently less melting than would be the case when ice dynamics were not included.

The disadvantage of using prescribed climate model output to drive an ice sheet model in "offline mode" (one-way coupling) is that changes in the ice sheet are unable to influence the climate, omitting potentially important feedbacks. For instance, changes in orographic height and surface albedo could alter atmospheric circulation (Toniazzi et al. 2004; Lunt et al. 2004), temperature, and precipitation. In addition, freshwater input to the ocean could change ocean circulation, with potential changes to the thermohaline simulation of particular concern (Cubasch et al. 2001). The latter effect was demonstrated by Fichefet et al. (2003), who coupled the Huybrechts Greenland ice sheet model to Laboratoire du Météorologie Dynamique–Coupled Large-scale Ice Ocean model (LMD–CLIO) and simulated the twenty-first century, including ocean freshwater input but not orographic height change. In the experiment, a strong and abrupt weakening of the North Atlantic thermohaline circulation occurs at the end of the twenty-first century. This feature is triggered by an enhanced freshwater input arising mainly from increased melting on the Greenland ice sheet. As a consequence of the circulation decline, a marked cooling takes place over eastern Greenland and the northern North Atlantic. This result underlines the potential role of the Greenland ice sheet in the evolution of climate over the twenty-first century.

In this paper we investigate the effects of a two-way coupling between the Greenland ice sheet model and an atmosphere–ocean general circulation model (AOGCM). Starting from preindustrial conditions the atmospheric carbon dioxide concentration will be quadrupled then stabilized while a long simulation of 3000 yr is performed. The resulting ice sheet, and the local and global climates, will be compared with the results from a simpler experiment with a prescribed ice sheet.

2. Model description

The third Hadley Centre Coupled Ocean–Atmosphere GCM (HadCM3) has an atmosphere resolution of 2.5° latitude \times 3.75° longitude and 19 vertical levels, and an

ocean resolution of $1.25^\circ \times 1.25^\circ$ and 20 vertical levels (Gordon et al. 2000; Pope et al. 2000). The model has been run successfully without flux correction for long periods. In the standard HadCM3 the ice sheets have fixed extent and orography, based on the United States Geological Survey (USGS) dataset (available online at <http://dss.ucar.edu/datasets/ds754.0/>), with a surface cover of deep snow. Variations in ice albedo as a result of surface snow aging and wetness are not included. Surface melting can occur on the ice sheet and the runoff is instantaneously mapped to river outflow points in the ocean component of HadCM3. Since standard HadCM3 has no ice sheet dynamics, there is no iceberg production. Instead, the climatological average of the simulated net surface mass balance of Greenland is spread as an equivalent flux of freshwater over a fixed area of the surrounding ocean, corresponding to the region in which icebergs are observed (Bigg et al. 1996; Gordon et al. 2000).

The three-dimensional Greenland ice sheet model (GISM) employed here has full thermo-mechanical coupling and includes a visco-elastic model of the solid earth to simulate the isostatic adjustment process (Huybrechts and de Wolde 1999). The GISM dynamics component includes ice deformation and basal sliding, but not deformation of subglacial sediment. The melt and runoff model is based on the degree-day method in which the surface melt is parameterized as a function of surface air temperature, rather than performing a detailed surface energy balance calculation. The precipitation fraction that falls as rain is also determined by the surface air temperature. The liquid water produced by the model (meltwater and rain), will at first refreeze and produce superimposed ice, the amount of which is determined by the heat required to raise the winter snowfall to the melting point. Subsequent liquid water will fill the pore volume of the snowpack until saturation is reached, after which runoff takes place (Janssens and Huybrechts 2000). The model is driven by monthly anomalies of 1.5-m temperature and by annual values of precipitation minus evaporation ($P - E$), interpolated on to the GISM model grid. The GISM calculates ice dynamics on a regular 20×20 km grid with 26 sigma levels. Although the GISM can be run offline using output from GCM simulations to drive it (one-way coupling) we have embedded it within HadCM3, in order to include the climate feedback mechanisms (two-way coupling). We will refer to the resulting composite atmosphere-ice sheet-ocean model as HadCM3-GISM, to distinguish it from standard HadCM3. Such a coupling of an ice sheet model has previously been undertaken with climate models of reduced complexity (Weaver et al. 1998; Yoshimori et al. 2001) or using an

AOGCM (Huybrechts et al. 2002; Fichefet et al. 2003), but with fixed Greenland orography. This is the first time a complete two-way coupling has been used with a complex climate model, and for a multimillennial period.

In these experiments HadCM3 is coupled to GISM once every model year. A schematic of the exchanges between HadCM3 and GISM is shown in Fig. 1. Monthly mean 1.5-m temperatures in HadCM3 are differenced from a 100-yr HadCM3 control climatology to produce temperature anomalies that are applied to GISM. The temperatures over Greenland in the HadCM3 control run, similar to many AOGCMs, do not compare well with observations. The central ice sheet winter temperatures are too cold by $\sim 10^\circ\text{C}$ (Murphy et al. 2002), and consequently, the use of monthly temperature anomalies rather than temperatures directly is required to eliminate climate model biases. As the ice sheet surface elevation changes during a simulation, the model temperatures must be referenced back to a fixed ice sheet orography to determine the true temperature anomaly, a process that requires an estimate of the surface temperature lapse rate. Relatively small changes in this lapse rate can introduce biases in the derived temperature anomaly. The surface temperature lapse rate over Greenland, which is driven by energy balance, was fixed at 8°C km^{-1} for the purposes of adjusting the changing surface elevation to climatology only. This is within the annual range in surface temperature lapse rate observed by Steffen and Box (2001). Free atmosphere lapse rates change within the AOGCM and are reflected in the temperature anomalies used for surface forcing. The monthly mean HadCM3 precipitation is applied directly as the climatology shows good agreement with current observations (Murphy et al. 2002).

After performing surface mass balance and ice dynamic calculation, GISM returns a new orography, ice surface runoff, basal ice melting, land surface runoff, and iceberg-calving mass flux, which are interpolated back to the HadCM3 grid. The new orography is used to check for changes in the ice mask such that a HadCM3 grid cell is deemed to have changed from ice covered to ice free or vice versa if a threshold of 50% cover has been passed. When this occurs, the parameters of the HadCM3 land surface scheme [Met Office Surface Exchange Scheme (MOSES); Cox et al. 1999] are modified appropriately, defining the surface albedo, roughness length, soil (dark clay) and dominant vegetation type (tundra), temperature, and moisture profiles. The orographic heights are updated and the orographic roughness characteristics, required by the HadCM3 boundary layer scheme, are recalculated. Runoff from

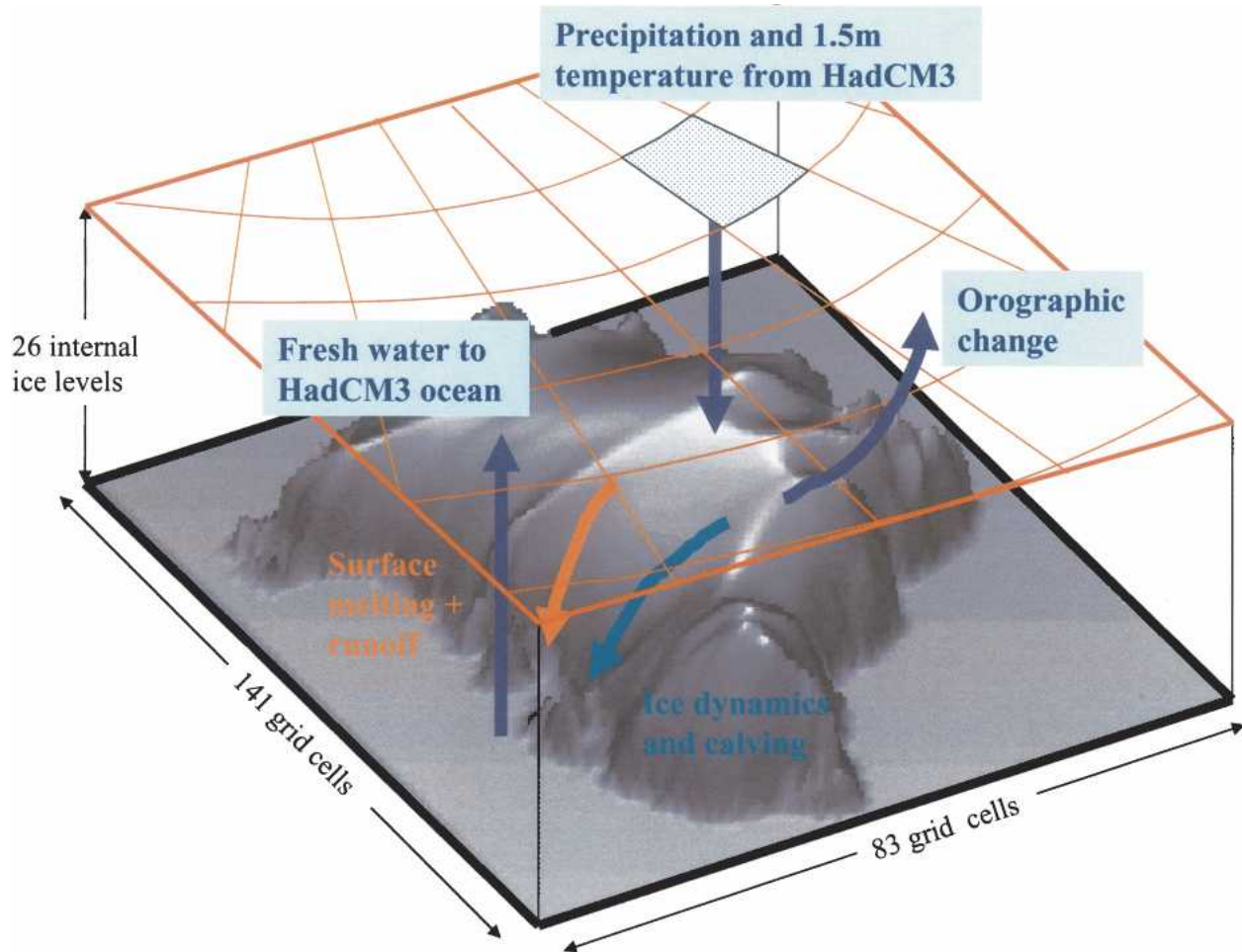


FIG. 1. Schematic of the coupling between (top grid) HadCM3 and (lower grid) GISM. Blue arrows denote field transfers, via an interpolative coupler, between HadCM3 and GISM.

Greenland is computed by the GISM surface melt and refreezing scheme where there is ice but the GISM land surface runoff is replaced by MOSES over the ice-free area. Since the river outflow points do not change significantly between ice surface and bedrock drainage basins, the outflow points were kept fixed as in standard HadCM3, and drainage to interior lakes was not allowed. The iceberg-calving flux in GISM is assumed to equal the flux of ice that crosses the grounding line, and is applied to the same region of the ocean as in standard HadCM3. The coupling of HadCM3–GISM conserves water within the system of atmosphere, land, and ice sheet but the ocean does not since it has a rigid lid and therefore a fixed volume.

For part of the coupled simulation an asynchronous technique was used in which 10 yr of the GISM were run for each year of HadCM3. This will not greatly affect the results because the additional impact of the ice sheet runoff on the ocean circulation was observed

in the synchronous part of the experiment to be negligible. In addition, the orographic changes, and consequent feedback from the atmosphere, were found to be slowly varying and continuous functions. Since the ice sheet integrates interannual variability, the asynchronous coupling will alter the power spectrum of ice sheet volume changes, tending to produce larger fluctuations over longer time scales. However, the fluctuations remain small compared with the forced change.

3. Design of Greenland deglaciation experiments

The purpose of the first set of experiments is to investigate Greenland deglaciation in a warmer future climate using the two-way coupled modeling approach. A total of four HadCM3 simulations and one GISM offline simulation are required.

1) Control1 (1800 HadCM3 yr): The standard

HadCM3 control run (Gordon et al. 2000; Pardaens et al. 2003), which has the atmospheric greenhouse gas composition appropriate to 1860. GISM is not included.

- 2) Control2 (150 HadCM3 yr): HadCM3–GISM control simulation, also with greenhouse gases appropriate to 1860. The initial state of the Greenland ice sheet is configured through spinning up the GISM for 225 000 yr (the last two glacial cycles) using perturbed $P - E$ fields from Control1 and spatially uniform temperature changes derived from ice cores. Control2 is required to obtain an internally equilibrated ice sheet model, and to determine the influence of the orography of GISM on the regional circulation.
- 3) GHG1 (1130 HadCM3 yr): This simulation uses standard HadCM3. The atmospheric carbon dioxide volume concentration is held constant at 1160 ppm, 4 times the preindustrial value. The climate warms rapidly to begin with, and then at a decreasing rate, but is not in equilibrium by the end of this simulation due to continuing deep-ocean warming (Gregory et al. 2004). The initial state of (greenhouse gas) GHG1 is produced by a preceding experiment, in which carbon dioxide is increased by $2\% \text{ yr}^{-1}$ for 70 yr starting from control1 (Thorpe et al. 2001).
- 4) GHG2 (735 HadCM3 yr, > 3000 GISM yr): This simulation uses HadCM3–GISM with a carbon dioxide volume concentration of 1160 ppm. It is initialized by incorporating GISM into the initial state of GHG1. After 350 yr of synchronous operation, the coupling is made asynchronous with 10 yr of ice sheet simulation for each year of HadCM3. The disequilibrium in the global mean temperature, due to the oceanic heat capacity, is statistically indistinguishable from that in GHG1.
- 5) ALONE (3000 GISM years): This simulation uses GISM alone driven by HadCM3 temperature anomaly and $P - E$ fields from the GHG1 simulation. As in the GHG2 experiment, asynchronous coupling was used after 350 yr. To a large extent this simulation emulates similar forward coupled experiments (Huybrechts and de Wolde 1999) so as to provide a baseline for comparison with two-way ice sheet coupling.

The change in climate variables resulting from the quadrupling of atmospheric carbon dioxide is given by (GHG2–Control2) for HadCM3–GISM and by (GHG1–Control1) for standard HadCM3. The impact of the GISM then follows as (GHG2–Control2) – (GHG1–Control1). That the surface temperature has not reached equilibrium in 3) and 4) is handled by com-

paring corresponding AOGCM years between the two cases.

4. Results and discussion of the Greenland deglaciation experiments

Using these experiments we address the following connected questions.

- 1) How does the GISM preindustrial ice sheet differ from the Greenland ice sheet of standard HadCM3?
- 2) How does the ice sheet evolve when coupled to the climate model?
- 3) Do changes in the Greenland ice sheet cause significant changes in local and global climate?
- 4) How important are the feedbacks between the ice sheet and climate to the evolution of the ice sheet?

a. How does the GISM preindustrial ice sheet differ from standard HadCM3?

At $840 \times 10^{12} \text{ kg yr}^{-1}$ HadCM3 has a similar total precipitation on Greenland to that indicated in the ECMWF reanalysis (Appenzeller et al. 1998). However, because of the low spatial resolution and consequently lower orographic slopes at the coast, the accumulation on the ice sheet, rather than the ice-free coastal region, is somewhat greater than that observed (about $695 \times 10^{12} \text{ kg yr}^{-1}$ versus $\sim 520 \times 10^{12} \text{ kg yr}^{-1}$; Church et al. 2001). The initial Greenland topography in Control2, which is calculated using the GISM model, implies a total ice sheet volume of $3.19 \times 10^6 \text{ km}^3$, 11% larger than recent estimates of its actual volume (Church et al. 2001). It nonetheless has a realistic form, and is within 100 m of that derived from the U.S. Navy surface orography, used in standard HadCM3, at the summit and most of the central region (Fig. 2). The largest differences are along the eastern margin, especially in the northeast and at the southern tip of Greenland, where the simulated topography reaches 500 m above the U.S. Navy orography. Differences of this size are enough to alter the atmospheric circulation through an increased blocking of the westerly flow. This, in turn, leads to changes in the pattern of mean sea level pressure with raised surface pressure on the western side and lowered surface pressure on the eastern downstream side. A consequence of this altered atmospheric circulation is a redistribution of sea ice, which brings about significant changes in surface air temperatures over the ocean (Fig. 3). The sea ice cover in the Labrador Sea increases, reducing surface air temperature, whereas the reverse happens in the Greenland and Barents Seas.

Ablation and calving in Control2 amount to 410×10^{12} and $300 \times 10^{12} \text{ kg yr}^{-1}$, respectively, which may be

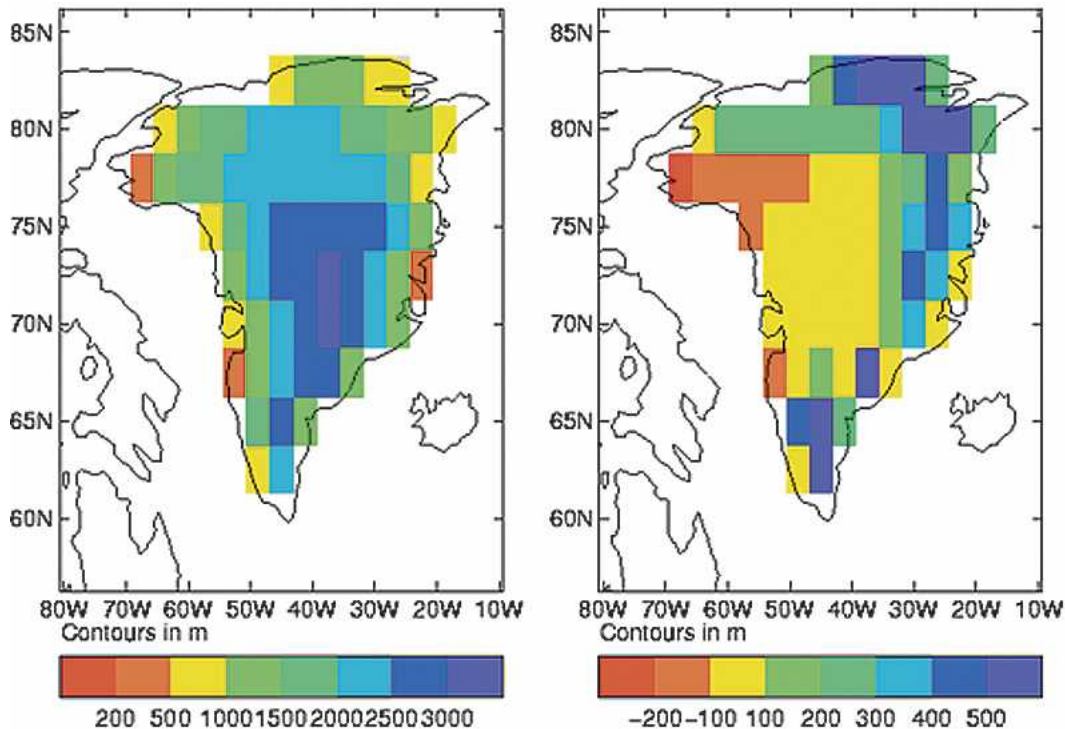


FIG. 2. (left) The standard HadCM3 Greenland orography based on U.S. Navy 10-min dataset, used in Control1/GHG1 and (right) its difference from the HadCM3-GISM orography, spun up using HadCM3 precipitation and 1.5-m temperature fields, used in Control2/GHG2.

compared with observationally derived estimates of 297×10^{12} and 235×10^{12} kg yr⁻¹ from Church et al. (2001). Hence HadCM3-GISM has roughly the right balance of liquid runoff and iceberg production. In standard HadCM3 (Control1) the calving is set to 488×10^{12} kg yr⁻¹ to close the mass budget.

b. How does the ice sheet evolve when coupled to the climate model?

Under a $4 \times \text{CO}_2$ climate forcing the Greenland ice sheet volume and area undergo a continuous reduction. By year 3000 less than 5% of the original ice sheet volume remains. The decline can be divided into four phases, which are shown in the volume change timeline in Fig. 4. The spatial evolution of the ice sheet mass is shown in Fig. 5.

- Phase 1: The ice sheet melts in the regions least constrained by coastal mountains (i.e., where the ice margin is near sea level), that is, the north and the southwest. The melt rate is so great in these relatively low-lying regions (>20 m yr⁻¹) that the ice undergoes considerable retreat at a constant rate for some 300 yr. Although the plateau has a net positive mass balance, the ice sheet as a whole has ablation 3 times

greater than precipitation. Volume and area decrease at the same fractional rate, because the ice sheet is contracting without losing height.

- Phase 2: Now having a steeper surface profile at the ice edge, coastward ice sheet dynamical flow increases, lowering some plateau regions below the equilibrium line. The southern summit starts to disappear and the ice sheet volume-to-area ratio decreases.
- Phase 3: On the western side of the ice sheet, the ice margin is not elevated (cooled) by mountain ranges, and as this margin moves inland the bedrock elevation decreases, accelerating ablation. The exception to this retreat is in the region of the western mountains at 72°N where the retreat is slowed resulting in a spur in the ice sheet in this region. The eastern mountains act as a barrier, restricting the dynamical flow of ice to lower elevation, and the ice here remains above the ablation zone throughout the simulation.
- Phase 4: The ice sheet retreats up the western flanks of the eastern coastal mountains reaching a new quasi-equilibrium maintained by the high elevation and increased local precipitation. The ice sheet is now so restricted in area that local climate variability has

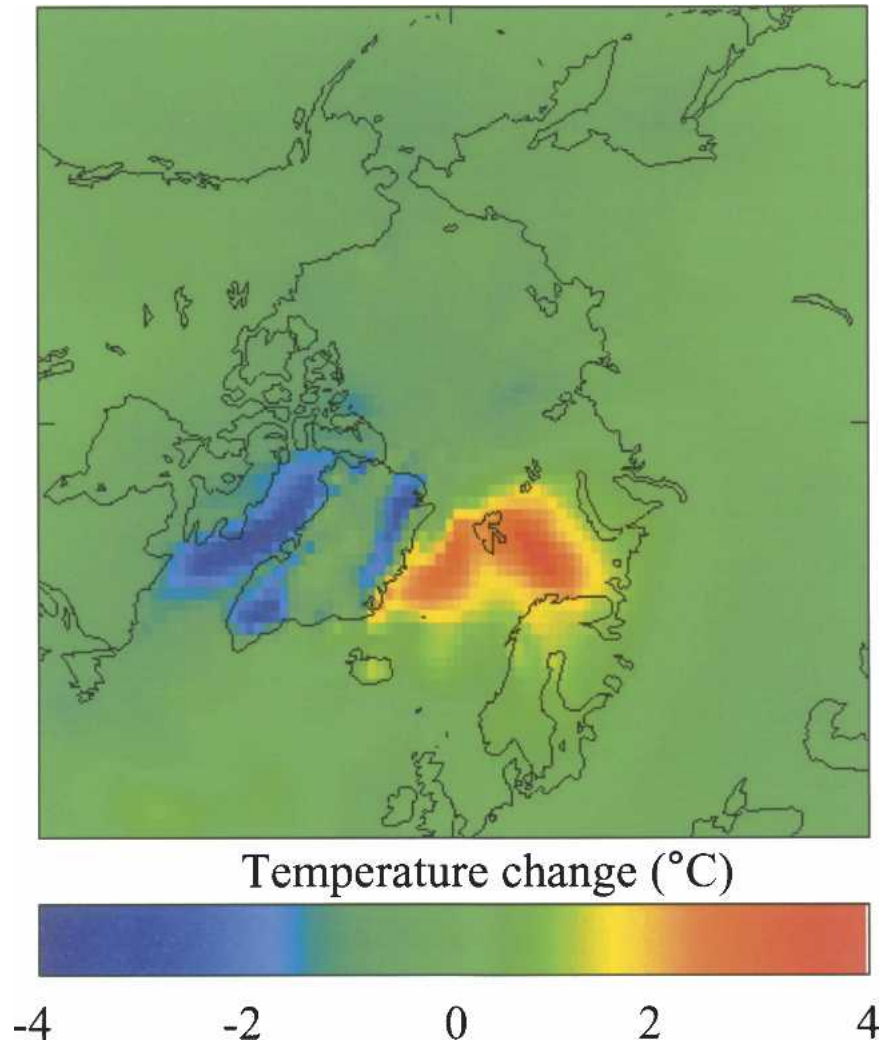


FIG. 3. The small difference in surface orography over Greenland between Control2 and Control1 results in a significant change in the annual mean 1.5-m temperature field. The orographic change (an increase in elevation resulting in the cooling of the ice sheet surface) alters the westerly flow and storm tracks, changing the winter sea ice cover, which consequently influences the surface temperatures.

a significant impact on it, and it declines slowly but with rapid bursts of ablation associated with regional increases in surface temperature. It reaches a further temporary equilibrium at 3% of its initial volume and 8% area, but then resumes a slow decline.

Changes in ablation, accumulation, and ice dynamics all play a role in the evolution of the ice sheet (Lefebre et al. 2002; Kilsholm et al. 2003; Payne et al. 2000), and we will consider each in turn.

In the first 150 yr, ablation increases by 65% to 2 m yr^{-1} of ice averaged over the ice sheet area—3 times greater than the precipitation—at which it remains for much of the simulation, but it declines absolutely with

the ice sheet area (Fig. 6). The large-scale positive degree-day melt parameterization used here for the Greenland ice sheet is highly sensitive to its parameters (standard temperature deviation, snow, and ice degree-day factors), which were obtained by calibrating the melt and runoff model against available present-day observations of equilibrium-line altitude, mass-balance transects, and global estimates of accumulation rate, calving rates, and bottom melting rates (Janssens and Huybrechts 2000). Lefebre et al. (2002) found that the snow and ice positive degree-day factors vary considerably over the ice sheet. At low elevations, their modeled snow degree-day factor closely approached the generally accepted value of 3 mm water equivalent

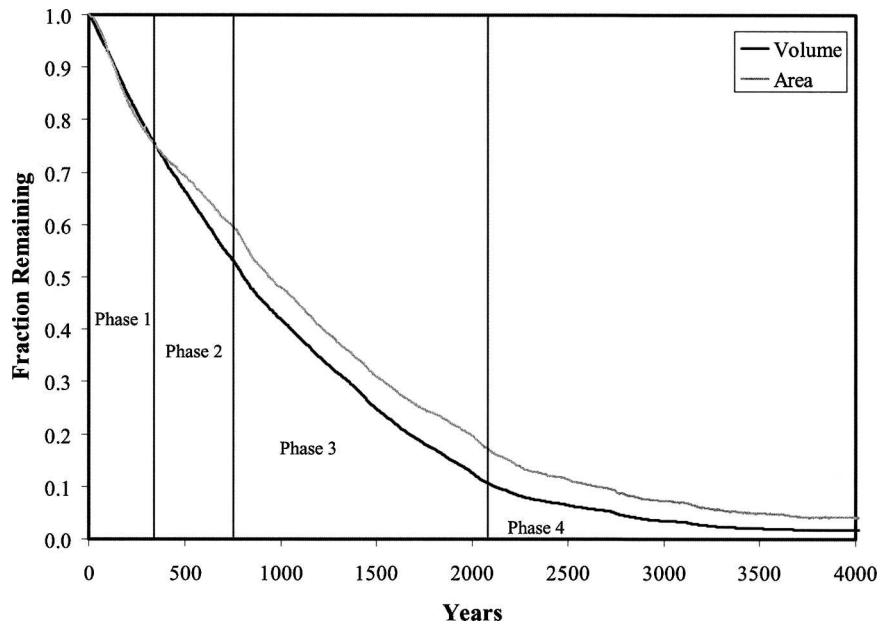


FIG. 4. The rates of change of ice sheet volume (dark line) and area (light line) during the GHG2 simulation. Different phases of the ice sheet evolution are described in the main text.

(w.e.) $\text{day}^{-1} \text{ } ^\circ\text{C}^{-1}$. Higher up the ice sheet, Lefebre et al. (2002) found large values up to $15 \text{ mm w.e. day}^{-1} \text{ } ^\circ\text{C}^{-1}$ were simulated. For ice melt, maximum values of $40 \text{ mm w.e. day}^{-1} \text{ } ^\circ\text{C}^{-1}$ were found. The snow and ice positive degree-day factor distributions were however shown to peak, at 3 and $8 \text{ mm w.e. day}^{-1} \text{ } ^\circ\text{C}^{-1}$, respec-

tively, which are the values used here. Refreezing is of small importance close to the ice sheet margin. Higher up the ice sheet refreezing considerably lowers the amount of net ablation (Janssens and Huybrechts 2000).

Observed accumulation rates can vary across the ice

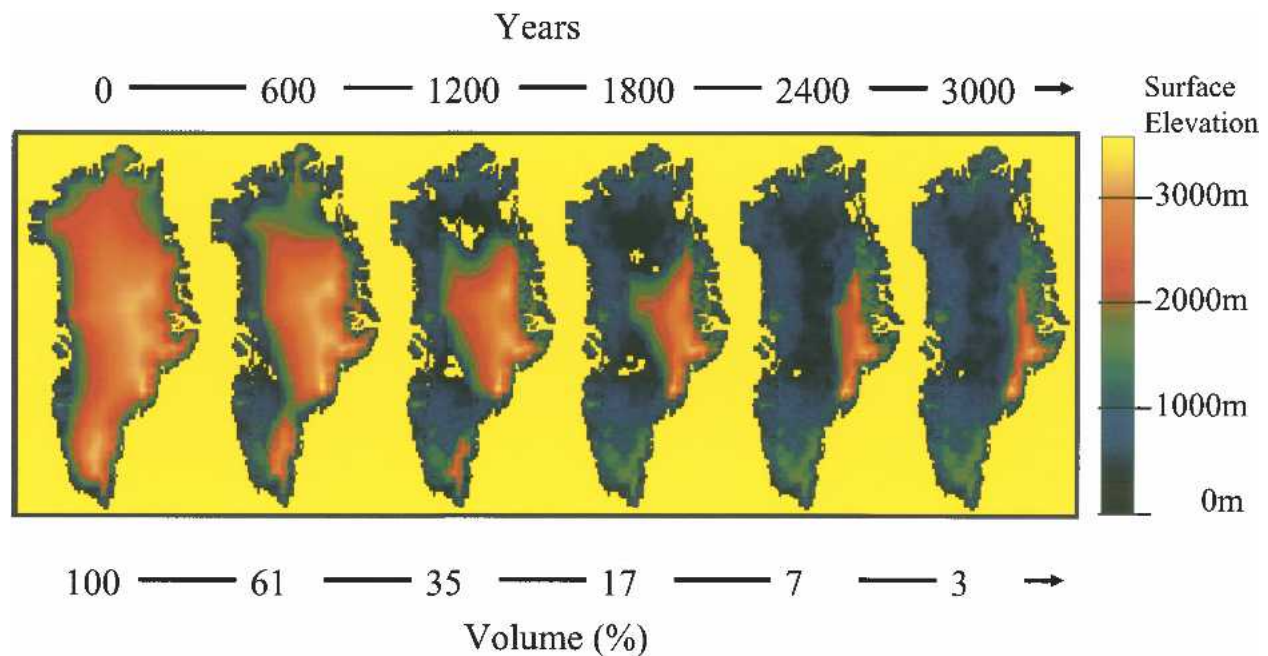


FIG. 5. The surface elevation for various snapshots of GHG2. Elevation is a combination of ice sheet thickness and bedrock height. Sea level is shown in yellow, with some inland regions starting below sea level, but rising above it as the bedrock rebounds.

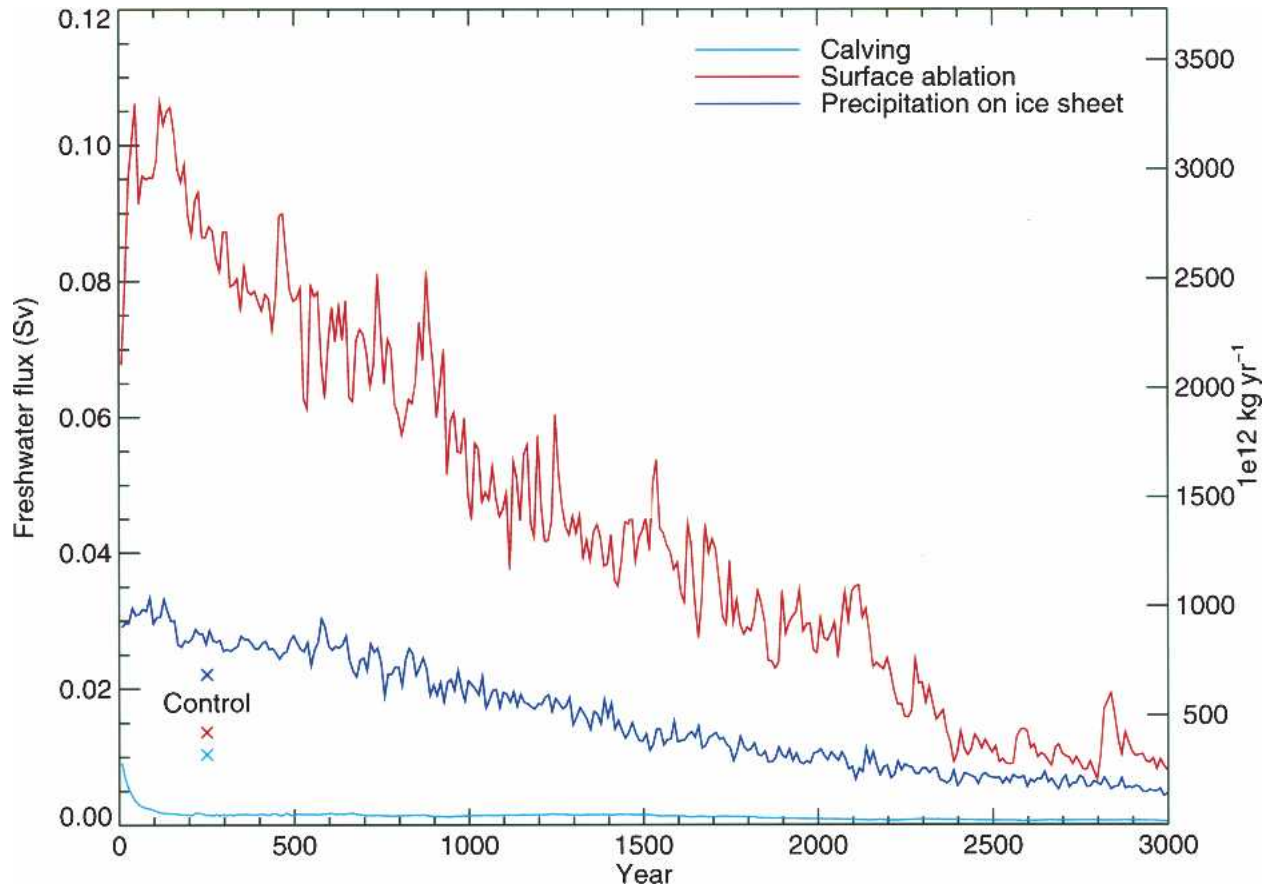


FIG. 6. The freshwater budget of Greenland ice sheet in GHG2, compared with the mean values from Control2. Surface ablation dominates the water budget, peaking at year 130. All component fluxes decline as the ice sheet area declines. The xs at the lower left show the levels of the different fluxes in Control2 for comparison.

sheet and also in time. Winter precipitation shows a low-frequency oscillation on a time scale of 100 yr that is likely to be due to changing circulation patterns (Anklin et al. 1998). Precipitation patterns have a strong dependence on the North Atlantic Oscillation (NAO) with the source regions for the precipitation changing from the North to east Atlantic as the NAO goes from a positive to a negative value (Schwierz and Davies 2002).

In the GHG2 simulation the area-average precipitation over Greenland increases in both GHG1 and GHG2 with respect to their controls for the first 400 yr (Fig. 7) as the climate warms. However, the increase in GHG2 is faster as the precipitation front follows the ice edge inland. The bedrock orography exposed as the ice sheet retreats is in general of low elevation, and consequently water vapor can move considerable distances inland following the retreat of the ice sheet edge before orographic lifting eventually results in precipitation. After 400 yr the annual precipitation over Greenland in GHG1 is 50% greater than the control (Control1), a

consequence of a warmer world and a stronger hydrological cycle. In GHG2, the Greenland precipitation continues to increase as the ice sheet declines, eventually reaching 90% above its control (Control2). In addition, the annual cycle of precipitation changes such that after 3000 yr, winter precipitation has remained constant, but the snow fraction has fallen from 94% to 88%. In summer total precipitation increases but the snow fraction has fallen from 37% to 17%, causing a small positive feedback on the rate of decline of ice volume. That the precipitating region has moved, in GHG2, from the ocean to land is shown in Fig. 7. The total precipitation falling over the ocean remains constant, after the initial warming, in GHG1 but declines in GHG2 by a few percent as the ice sheet shrinks and the precipitation front moves inland.

Ice dynamics are at first a counteracting effect in the sense that ice sheet disintegration proceeds slower than in experiments where ice dynamics are not allowed to react to changes in the ice sheet geometry. The mechanism involves a steepening of the margin in response to

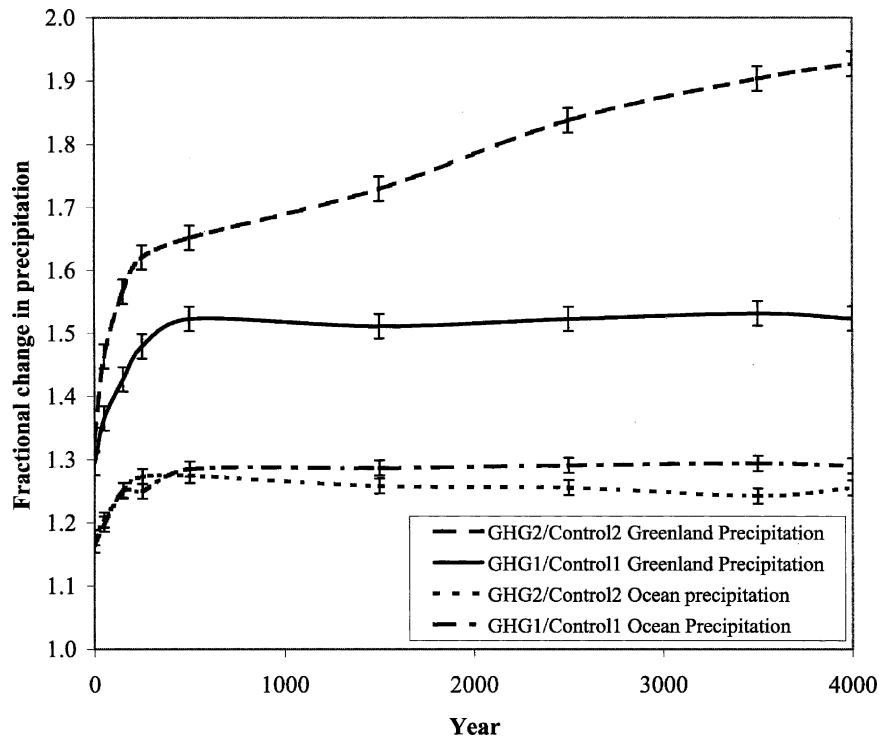


FIG. 7. The time series of fractional change in precipitation during GHG1 (solid line) and GHG2 (dashed line) with respect to their controls Control1 and Control2 for the Greenland region (increasing precipitation) and the adjacent ocean (decreasing precipitation). Error bars show 95% confidence limits based on the interannual variability.

increased balance gradients, much as described in Huybrechts and de Wolde (1999) and Huybrechts et al. (2002). The larger ablation rates at the margin combined with higher precipitation rates on the central plateau also allow for a larger height-to-width ratio that is fundamental to sustain the high elevation of the central plateau during the first few hundred years of the simulation. It is only after phase 1 that this balance can no longer be sustained and increased outflow eventually becomes larger than central accumulation rates, resulting in a drawing down of the central plateau. This makes the ice sheet more vulnerable to the imposed warming through the height–mass balance feedback as a larger fraction of the ice sheet ends up below the equilibrium line and can subsequently waste away. As the ice margins retreat from the coast, calving rates approach zero (Fig. 6).

c. Do changes in the Greenland ice sheet cause significant changes in local and global climate?

Here we compare the differences between the GHG1 simulation and Control1, and GHG2 and Control2. Atmospheric changes are discussed first, then ocean changes.

Global mean 1.5-m air temperatures initially rise, relative to the preindustrial control, but are very similar in the two simulations, reaching $+6.5^{\circ}\text{C}$ by year 500 in both GHG2 and GHG1 (Fig. 8). Over Greenland the warming is greater in both simulations than the global mean value, in line with the amplification of warming at high northern latitudes (Holland and Bitz 2003). A significant difference is caused by the inclusion of the ice sheet changes, with the contraction of the ice sheet in GHG2 leading to an enhanced surface warming over Greenland. The strongest initial warming, of more than 10°C , occurs along the margins where the ice sheet has retreated and exposed low-lying land (Fig. 9). Geographically, the largest increases in temperature in GHG2 occur along the northern Greenland coast and are probably enhanced due to the summer retreat of sea ice from this coast. After 3000 yr, the average temperature rise over Greenland is 18.8°C in GHG2, compared with 10.3°C at the end of GHG1. The removal of the ice sheet results in a temperature increase of 7.8°C in winter and 13.1°C in summer. This enhancement is due to a combination of lower surface elevation and reduced albedo (Crowley and Baum 1995; Toniazzi et al. 2004; Lunt et al. 2004). As the GHG2 ice sheet retreats up the eastern mountains, its mean surface eleva-

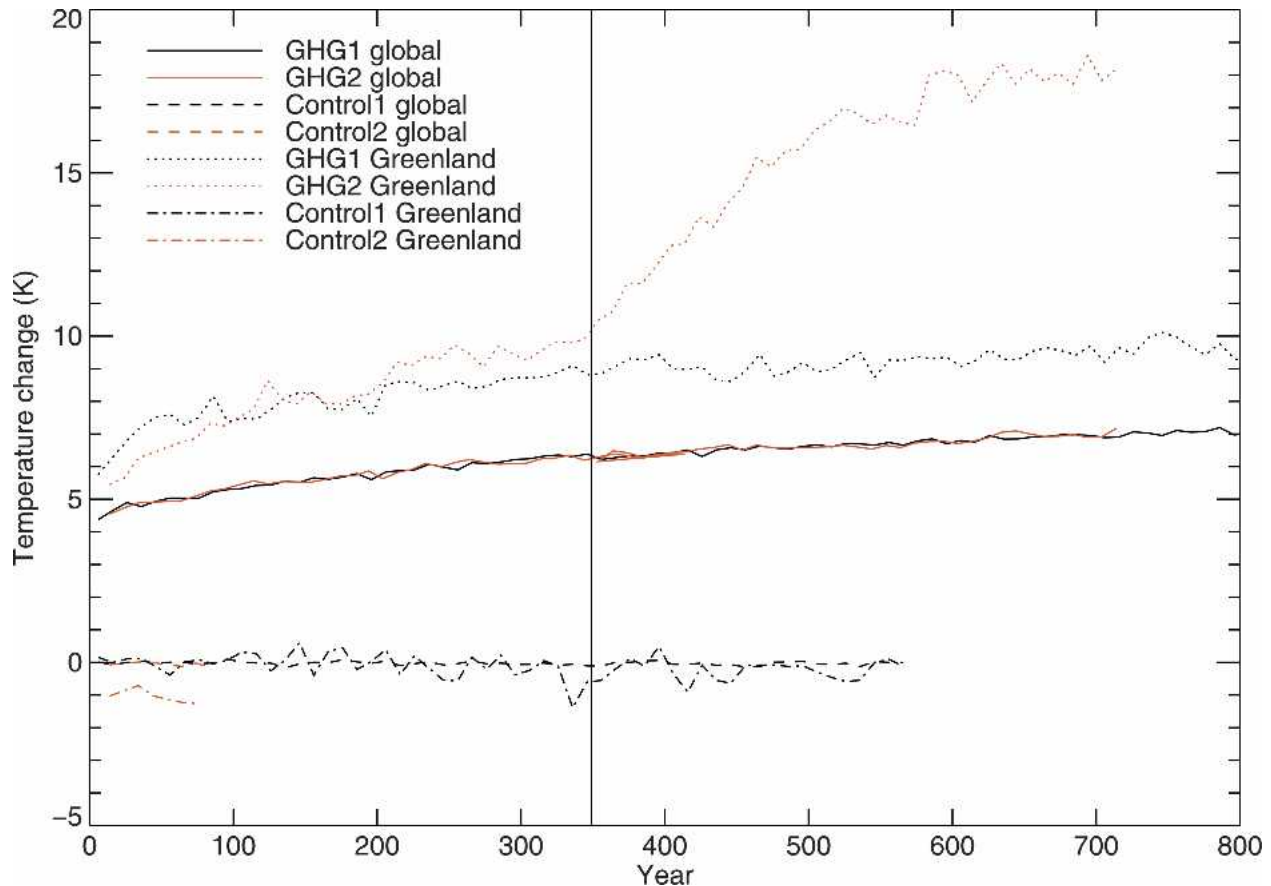


FIG. 8. Annual mean 1.5-m temperature changes with respect to preindustrial control, Control1. The global temperatures continue to rise, in both GHG1 and GHG2, as the ocean approaches equilibrium with the atmosphere. Changes in the Greenland ice sheet in GHG2 do not have a significant global impact as the temperatures remain identical to that in GHG1. The vertical line shows the transition between synchronous and asynchronous simulation in GHG2. The Greenland mean temperature in Control2 is colder than Control1 because the mean surface orography is ~ 100 m higher in Control2. Similarly, GHG2 starts colder than GHG1 for Greenland, but becomes warmer as the ice sheet elevation decreases and the ice sheet shrinks.

tion remains constant, but there is a slight drop in mean surface temperature (Fig. 10).

Using the four experiments available, it is not possible to distinguish between temperature increase from elevation–temperature feedback and albedo–temperature feedback. However, a simplistic analysis, which ignores possible changes in heat transport into the region, would attribute the winter temperature increase to elevation changes and the difference between winter and summer temperature rises to albedo changes. Such an analysis indicates that the two temperature feedback mechanisms are comparable in magnitude.

The change in surface albedo drives a change in the local atmospheric circulation during the summer, which acts as a negative temperature feedback. We hypothesize that the increase in summer surface temperature in the ice-free regions drives convection generating a

local circulation by increasing landward surface winds from the surrounding ocean (Fig. 11). The rising air results in atmospheric descent over the ice sheet warming the high elevation ice sheet, which is too cold for it to enhance ablation, and generates katabatic winds that cool the lower regions. A cooling of the ice margin reduces the ablation rate. The evidence for this summer circulation pattern in HadCM3 is provided by analysis of the circulation after 3000 yr. The ice-free area displays several regions (a few model grid cells in area) of reduced surface air pressure (~ -5 hPa) and increased surface air temperature, indicating an ascending air mass. Coincident with the changes in the ice-free region, surface air pressure over the ice sheet increases by ~ 3 hPa and the surface cools by $\sim 1^\circ\text{C}$. Low- and high-altitude winds reflect these surface pressure changes, as indicated by the maps of wind divergence at year 3000 in Fig. 12. An area of wind divergence at high model

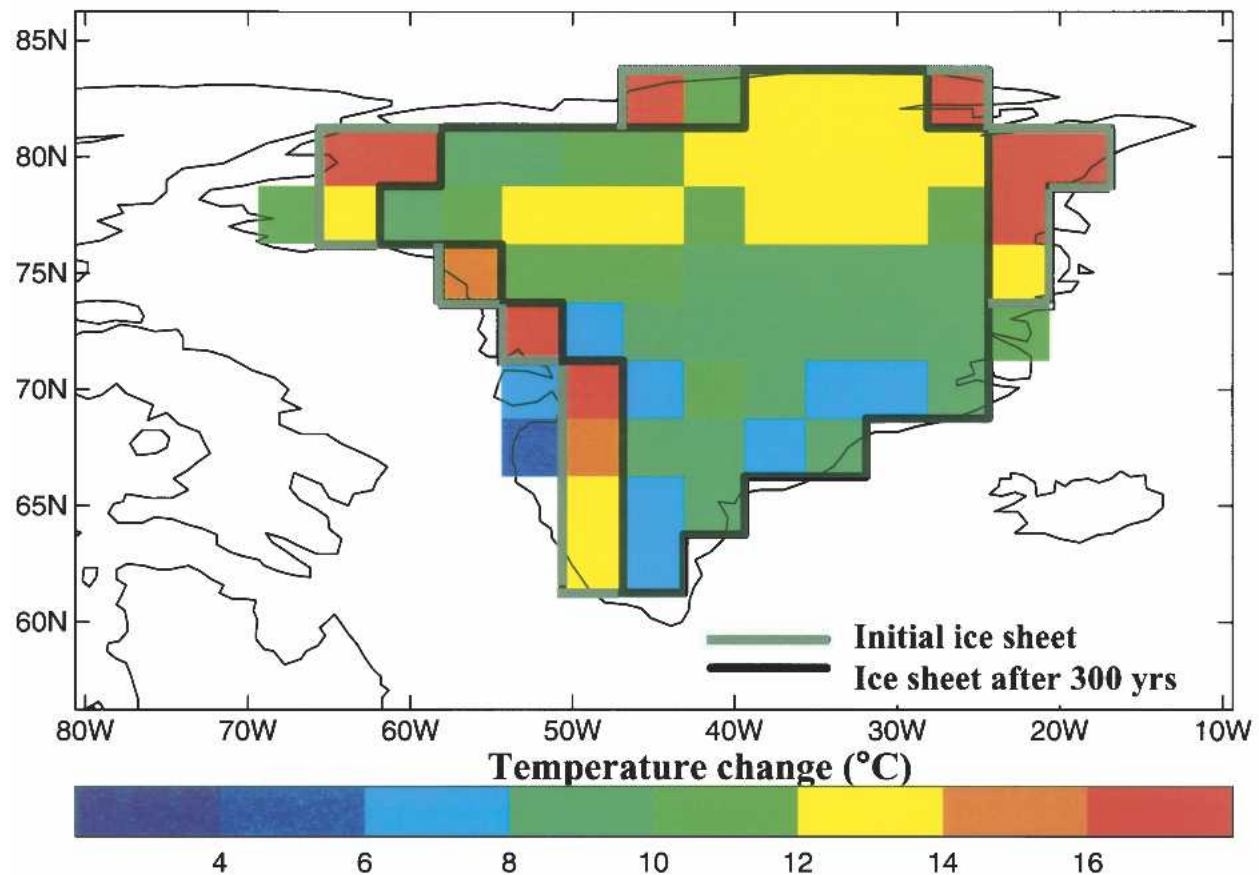


FIG. 9. Spatial changes in surface temperature after ~ 300 yr of GHG2 with respect to Control2. Main changes are around the edge of the ice sheet where ablation is highest and slopes are steep. Enhanced warming in the north is due to an absence, in GHG2, of the summer sea ice that is present in Control2.

levels combined with convergence at low model levels, indicates airmass ascent, and the reverse for descent. The regions of atmospheric ascent correlate well with increased surface temperature and follow the retreat of the ice edge in their general location. We suggest that the development of the circulation cells may be triggered by a minimum ice-free region, and consequently may be a function of GCM spatial resolution. The development of the circulation cells marks a change in the time development in the pattern of ice sheet ablation.

The regional scale shows surface pressure changes associated with changes in the westerly flow north of Iceland, a response in the stationary Rossby waves to orographic forcing (Cook 1992), which result in a shift in the polar front (Fig. 13) and a southerly shift in the mean storm tracks. The reduction in surface temperature results in an increase in winter sea ice cover in the Barents Sea with a consequent positive feedback and further surface cooling. There is no summer sea ice in the Arctic in these simulations, and the small temperature changes relate directly to sea surface temperature.

The change in the Barents and Labrador Seas following a decrease in the mean surface elevation of Greenland, is opposite in sign to the impact of the slight increase in elevation due to the initial conditions (Fig. 3). There is no evidence for significant effects on the climate of Europe or farther afield, except for a winter cooling of northern Scandinavia, due to the elimination of the ice sheet in line with the results of Toniazzi et al. (2004) and Lunt et al. (2004).

The deglaciation of Greenland increases the freshwater flux into the ocean from runoff, basal water, and icebergs. In addition, freshwater components arising from rain and snowfall on the parts of Greenland not covered by the ice sheet, which always run off, will increase as the ice sheet area declines. In GHG1, the freshwater flux stabilizes quickly at around 1700×10^{12} kg yr $^{-1}$, equivalent to about 0.06 Sv (1 Sv $\equiv 10^6$ m 3 s $^{-1}$). In GHG2, calving falls to near zero in the first century of the experiment, while the large increase in ablation gives a total freshwater flux of about 3500×10^{12} kg yr $^{-1}$ (0.12 Sv), about twice the size of that in GHG1.

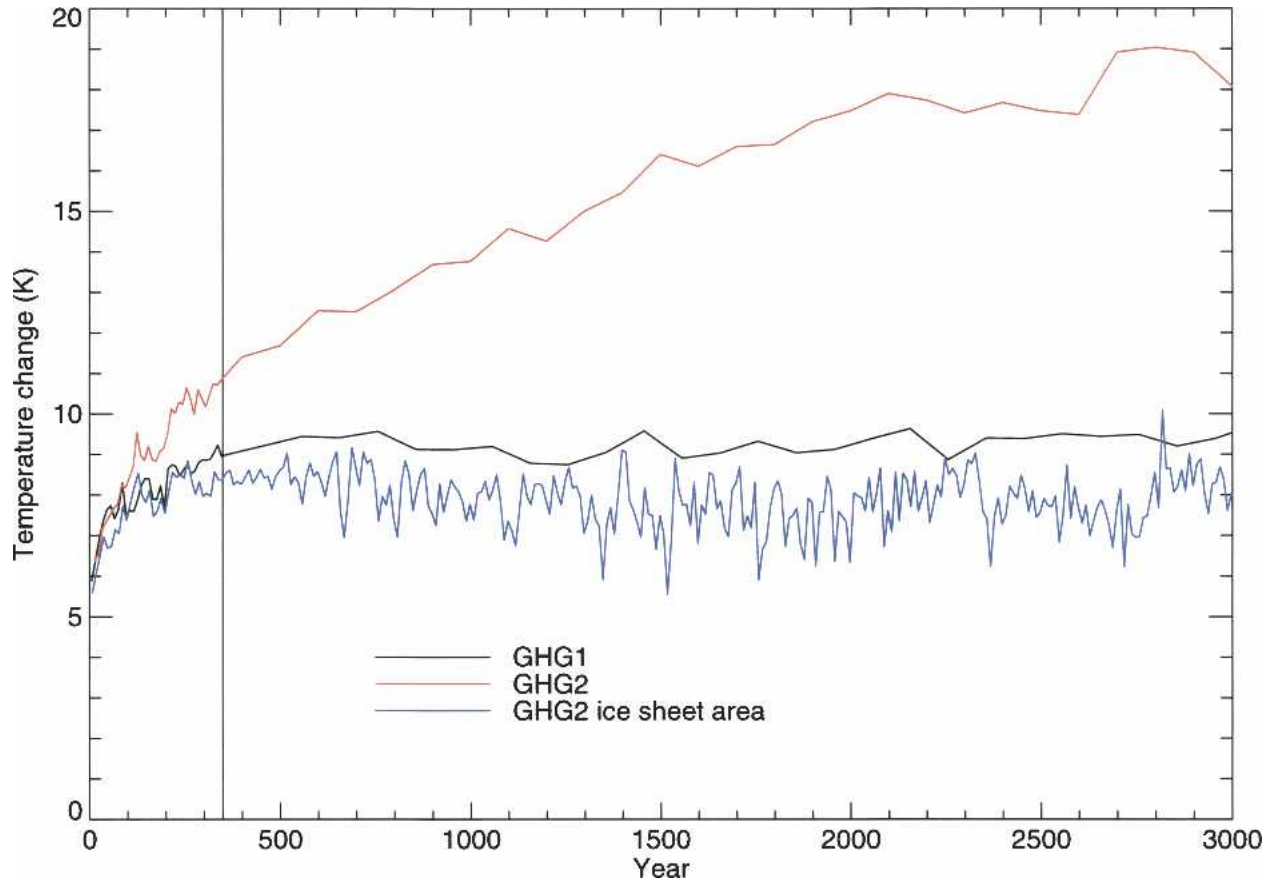


FIG. 10. Changes in mean annual surface air temperature with respect to the preindustrial control. All Greenland temperature rises in GHG2 as the surface elevation and albedo decline. The ice-covered region maintains a constant temperature as with large balance gradients the ice margin becomes steeper and the aspect ratio larger, with the result that for a smaller area it maintains more or less the same mean elevation. The vertical line indicates the change from synchronous to asynchronous coupling in GHG2.

This difference is due to the much higher ice sheet resolution of GISM and the use of different mass-balance schemes (surface mass balance in GHG1, degree-day in GHG2). As the ice sheet volume declines, surface ab-

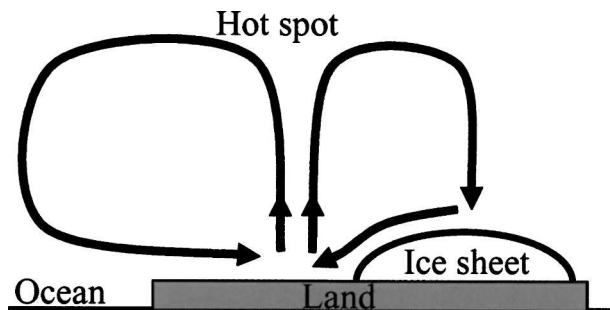


FIG. 11. Schematic of a summer local circulation system that evolves over Greenland as larger ice-free regions develop. A hot spot forms in the ice-free region warming the air, which rises. Descent over the ice sheet brings warmer air to the high elevations, but downslope winds bring cooler air to the ablation zone.

lation in GHG2 also declines such that after 2000 yr the freshwater flux in GHG2 has fallen to the same level as in GHG1.

One effect of the freshwater input from Greenland is a rise in global average sea level. The direct contribution of the extra water in GHG2 over 3000 yr is around 7 m, with half of this occurring in the first 850 yr. The rate of sea level rise is at a maximum near the start of the experiment, reaching around 5 mm yr^{-1} . For comparison, the twentieth-century rate of sea level rise is between 1 and 2 mm yr^{-1} , of which less than 0.4 mm yr^{-1} is from Greenland (Church et al. 2001).

There is the possibility that the freshwater from Greenland (Fig. 10) could modify the Atlantic thermohaline circulation (THC) because the freshwater alters high-latitude ocean density, on which the strength of the THC has been shown to depend (Stommel 1961; Rahmstorf 1995; Rind et al. 2001). Such a relation between THC strength and the meridional gradient of column-integrated density between 30°S and 60°N

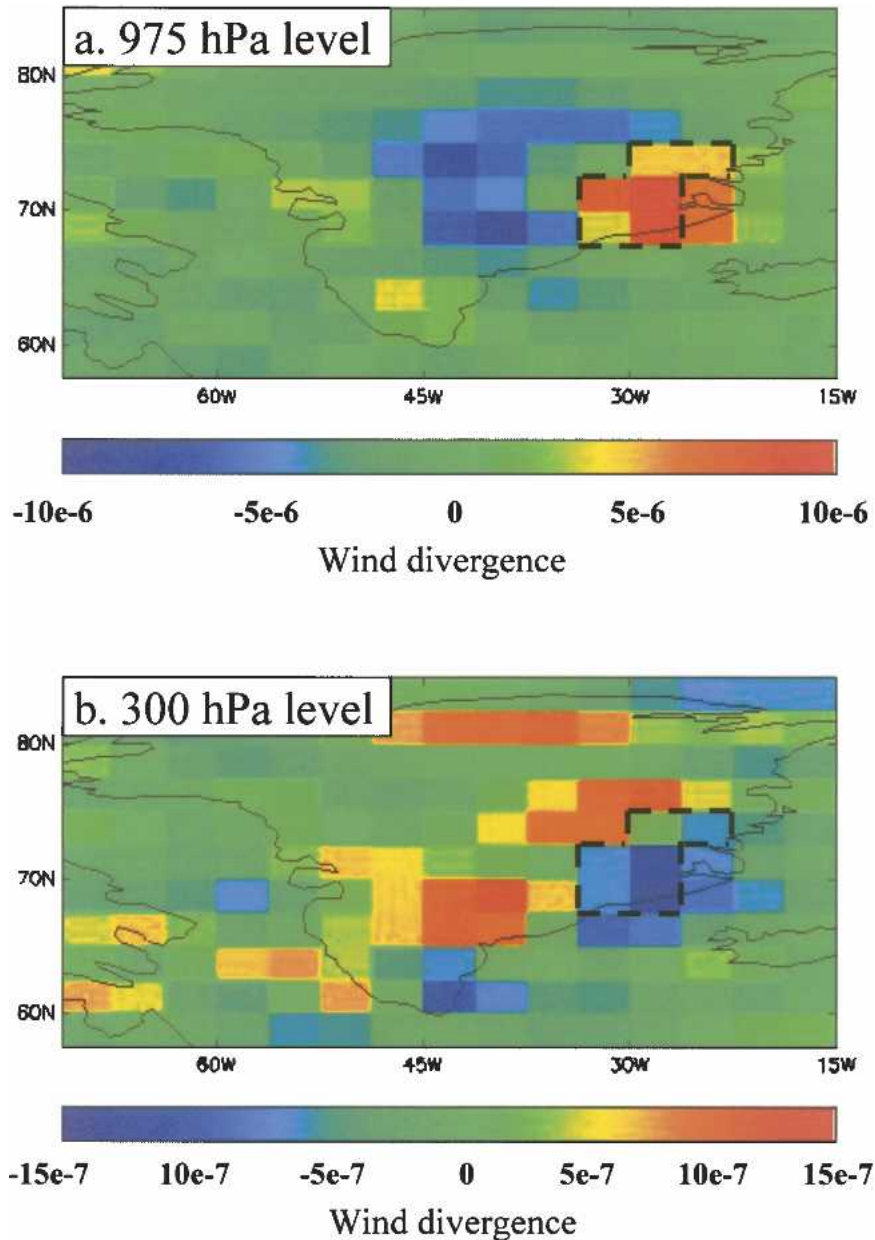


FIG. 12. The HadCM3 wind divergence over Greenland in year 3000 at (a) the low level (975 hPa) and (b) upper level (300 hPa). Divergent winds (red colors) at low levels and convergent (blue colors) at high levels indicate atmospheric ascent. The inverse conditions indicate descent. Regions of ascent correlate well with high surface temperature (ice free) and descent with the ice sheet (outlined region). Dotted lines show the extent of the ice sheet.

was found by Thorpe et al. (2001) for HadCM3. In both GHG1 and GHG2 the THC strength does decline, as measured by the maximum of the Atlantic overturning streamfunction (Fig. 14). The peak freshwater flux is greater in GHG2 than in GHG1 by about 0.06 Sv around year 130, producing an extra 1–2-Sv decrease in the THC. However, as this difference reduces, the THC in GHG2 recovers toward the value of

GHG1. This suggests that in HadCM3 a freshwater flux of at least 0.1 Sv is required to sizably alter the THC, which is consistent with other sensitivity tests done with this model, and also with some other state-of-the-art models. By contrast, Fichefet et al. (2003) found a reduction in the thermohaline circulation of 7 Sv in their model, for a freshwater input of only 0.015 Sv during the twenty-first century, producing a stronger

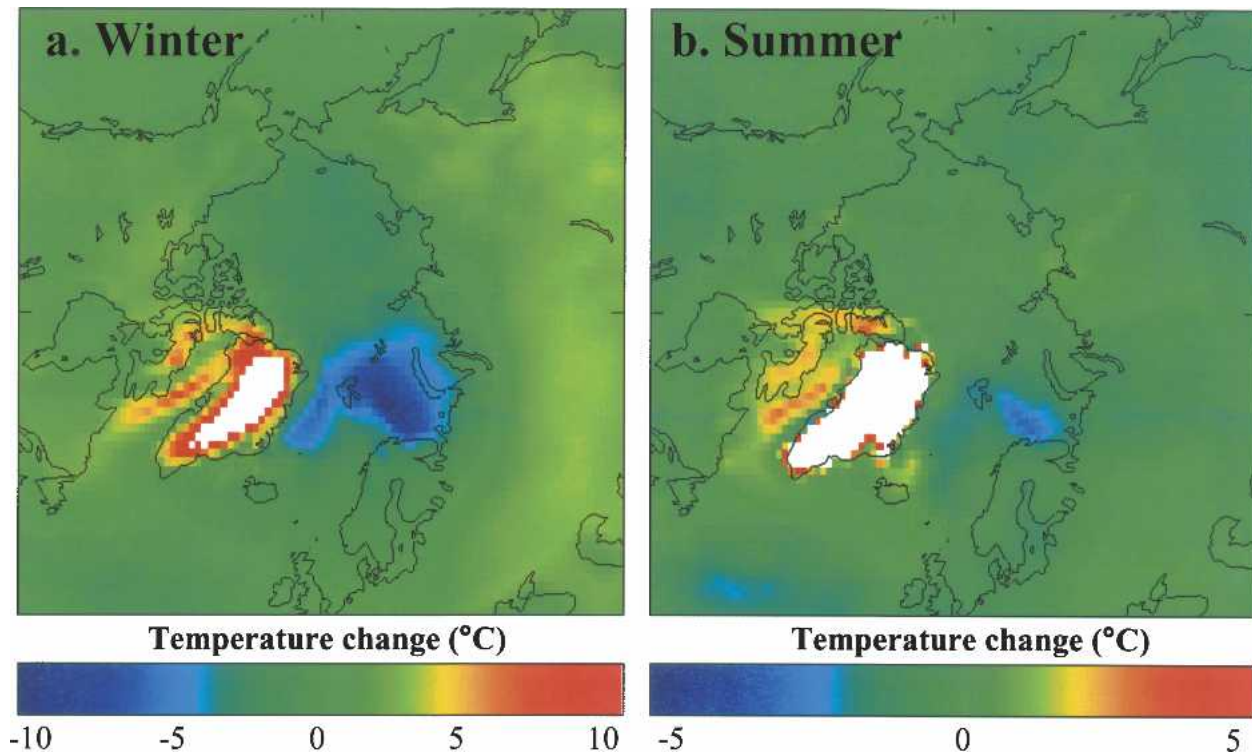


FIG. 13. The temperature differences between GHG2 and GHG1, showing the impact of the loss of 95% of the ice sheet for (a) winter and (b) summer. Westerly flow across Greenland rather than around the southern tip changes the storms to a more southerly track, reducing the flow of warm air into the Barents Sea. Sea-ice feedback as well as stronger storms in winter enhances the cooling in this region (sea ice cover is absent from the Arctic during summer). White regions indicate areas where the temperature change is greater than $+10^{\circ}\text{C}$.

coupling between ice sheet and climate change than in HadCM3.

d. How important is the interaction between the ice sheet and climate to the evolution of the ice sheet?

In the previous section we saw how changes in the ice sheet can alter the climate. Here, we investigate how allowing these additional changes in the climate can alter the ice sheet further by comparing the GHG2 results with those of ALONE. When the stand-alone model is forced with GHG2 temperature and precipitation fields the resultant ice sheet is identical to that in GHG2. The time series of ice sheet volume for these experiments are compared in Fig. 15. The two ice sheet simulations follow the same rate of decline until around a third of the ice sheet has been lost at around 500 yr into the simulation, at which point the ALONE ice sheet starts melting at a faster rate than that in GHG2. This leads to the ice sheet in GHG2 taking 500 yr longer to decline to 10% of original volume than in ALONE. Thus, the local climate change resulting from

the loss of the ice sheet has a negative feedback on its decline.

The reduction in the rate of decline of the ice sheet when climate feedbacks are included is likely to be a combination of reduced melting and enhanced precipitation. We already know from Fig. 6, that ablation dominates the mass balance at $4 \times \text{CO}_2$ but we still need to estimate their relative importance as climate-ice sheet feedback mechanisms. Applying the precipitation forcing from GHG2, which increases as the ice margin retreats, to the ice sheet in ALONE, results in a delay of only 80 yr in deglaciation to 10% of original ice volume (Fig. 15). Decreasing the annual mean anomaly temperature forcing in ALONE by 1°C reduces the mean ablation rate and the time for the ice sheet to decay to 10% is increased by 500 yr to that in GHG2. This indicates that differences in ablation, not precipitation, dominate the feedback processes. The ablation rates are identical in ALONE and GHG2 for the first 300 yr, after which they diverge, suggesting a gradually evolving temperature feedback process that acts to progressively cool the ice sheet as it declines in volume.

The principal candidate for cooling of the ice sheet,

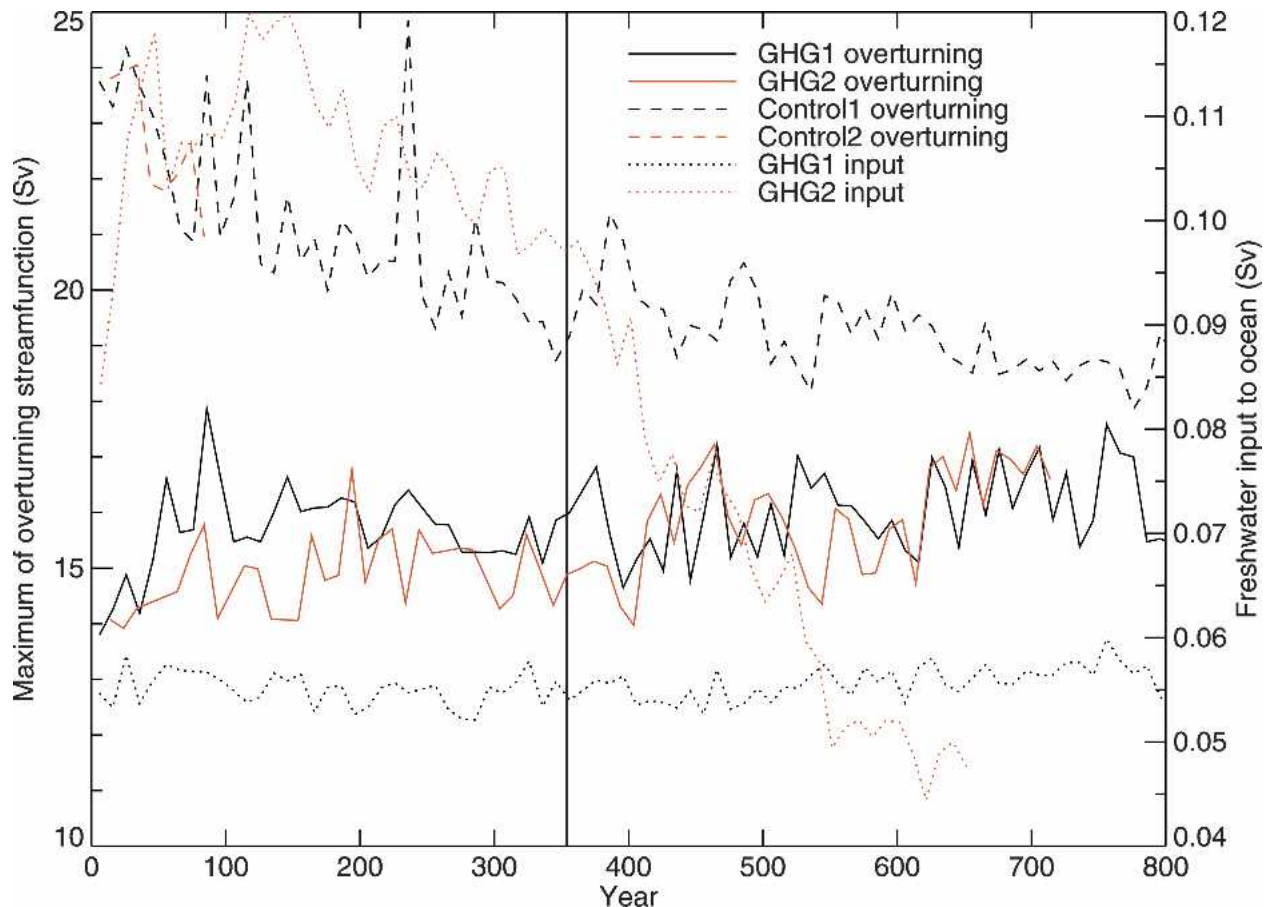


FIG. 14. Changes in the decadal mean thermohaline circulation over time. The control runs show similar strengths indicating that runoff patterns from the slight difference in orography is of little consequence. The greenhouse gas runs show a weakened overturning in GHG2 over GHG1 resulting from an increase in freshwater flux into the ocean (peaking at year 130 at 400% of that in GHG1), but a full recovery has been achieved by year 400. The vertical line at 350 yr indicates the change from synchronous to asynchronous coupling in GHG2.

and reduction in ablation rate, is the thermal circulation feedback at the ice sheet margin where the temperature contrast between land and ice is strong, the mechanism suggested in section 4c and Fig. 11. We have shown that the net cooling required to reproduce the lower ablation rate in GHG2 over that in ALONE is $\sim 1^{\circ}\text{C}$, equal to that observed through changes in the AOGCM atmospheric descent over the ice sheet (Fig. 10). An increase in precipitation has a minor influence on the ice sheet mass balance after year 1000, and is likely due to larger-scale circulation changes than that described here.

5. Conclusions

In this paper we have coupled a high-resolution dynamic ice sheet model to a coupled climate model and simulated the evolution of the ice sheet and climate over 3000 yr, with 4 times preindustrial atmospheric

carbon dioxide concentrations. A two-way coupling is used so that changes in the climate alter the ice sheet and changes in the ice sheet can further alter the climate. In this experiment the mass loss by runoff is the dominant ice process. The major ice-dynamic contribution is due to the changing driving stress (ice thickness and surface slope). Isostatic rebound is too slow to cause an appreciable reduction of marginal melting rates. At the end of the experiment only 7% of the original ice volume remains and is situated at the top of the eastern mountain range. The loss of ice volume is equivalent to a global average sea level rise of around 7 m, with a peak rate of rise of 5 mm yr^{-1} . The initial rapid surface melting of the ice results in a peak freshwater flux into the Atlantic after 130 yr of simulation, which causes a temporary 1-Sv decline in the thermohaline circulation. However, the circulation has fully recovered after 300 yr.

Apart from the sea level rise, the ice sheet changes

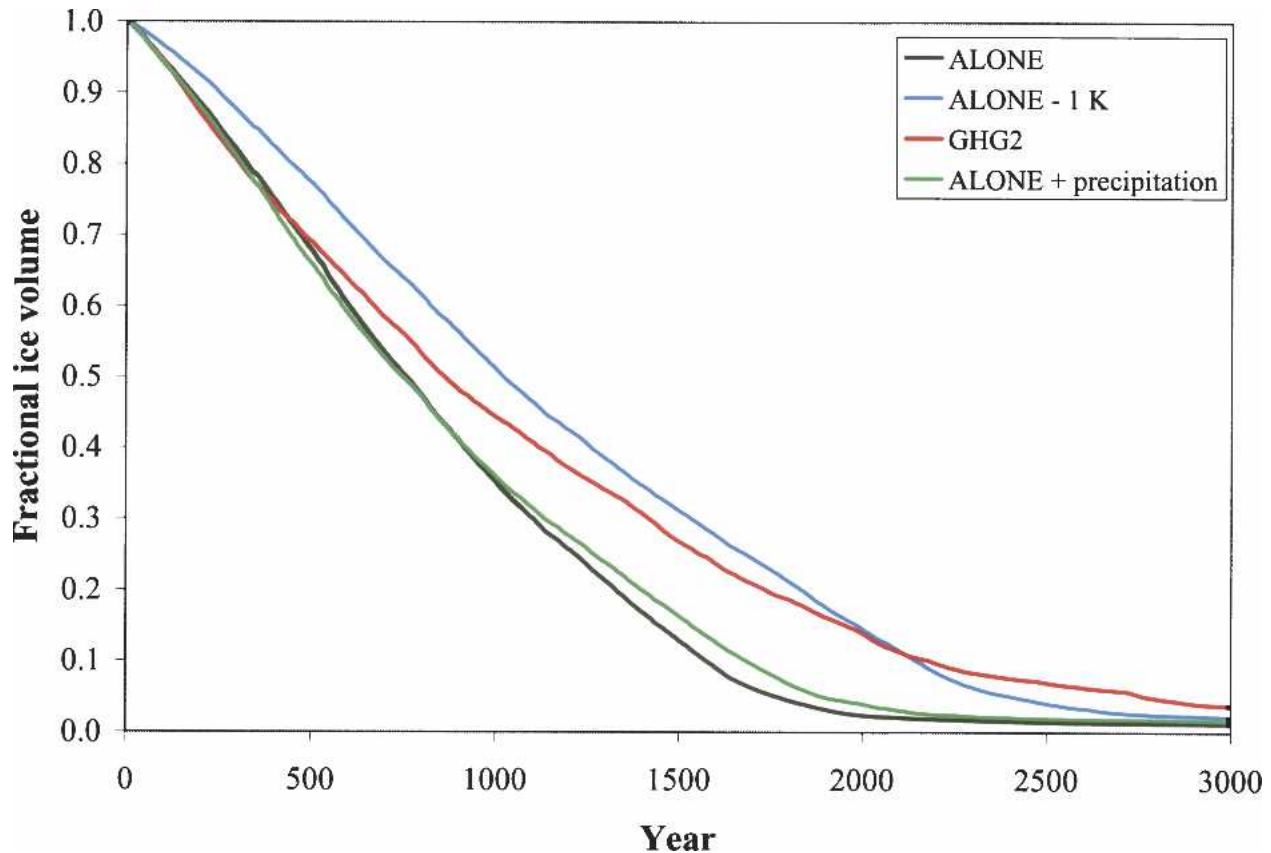


FIG. 15. The ice sheet volume evolution under forcing by GHG1 (ALONE) and GHG2 (precipitation and 1.5-m temperature anomalies). ALONE (black) produces a more rapid decline in the ice sheet volume. Forcing ALONE with the spatially different GHG2 precipitation (green) has only a small impact on the melt rate. If the ALONE temperature forcing is reduced by 1°C (blue) the mismatch with GHG2 (red) is poor in the initial stages of melt, suggesting that the difference between the two ice sheets is not a gross bias in surface temperatures, but that the temperature difference develops with time through a climate feedback mechanism.

appear to have little effect on global climate. However, locally they are significant and alter temperature, atmospheric circulation and precipitation. Orographic changes alter the stationary Rossby wave pattern, moving the polar front in the region of Svalbard southward and resulting in a cooling of the Barents Sea, enhanced by an associated extension of the winter sea ice cover. The peak Greenland precipitation follows the retreating ice sheet edge. Furthermore, as the ice sheet declines winter precipitation increases and alters the annual cycle of precipitation from one with a summer maximum to a much flatter annual cycle. With more winter precipitation more snow accumulates slowing the decline of the ice sheet. The increase in Greenland mean surface temperature over that in a model without two-way ice sheet–climate feedback is primarily due to a surface albedo–temperature feedback. A summer increase in surface heating generates a weak mesoscale atmospheric circulation in the form of atmospheric ascent in the ice-free area with descent over the ice sheet.

This thermal convective effect has a negative temperature feedback on the decline, inducing an enhancement of the descent of cold air into the ablation zone. Estimates using “offline” ice sheet models, which omit climate–ice sheet feedbacks, should thus be treated with caution when large changes in the ice sheet occur.

Acknowledgments. This work was supported by the U.K. Department for Environment, Food, and Rural Affairs under Contract PEDC 7/12/37, and through the German HGF-Strategiefonds Projekt 2000/13 SEAL (Sea Level Change) and the Belgian Science Policy Office Second Programme on Global Change and Sustainable Development under Contract EV/10/9B. We thank the anonymous referees for their helpful contribution to this work.

REFERENCES

- Anklin, M., R. C. Bales, E. Mosley-Thompson, and K. Steffen, 1998: Annual accumulation at two sites in northwest Green-

- land during recent centuries. *J. Geophys. Res.*, **103** (D22), 28 775–28 783.
- Appenzeller, C., J. Schwander, S. Sommer, and T. F. Stocker, 1998: The North Atlantic Oscillation and its imprint on precipitation and ice accumulation in Greenland. *Geophys. Res. Lett.*, **25**, 1939–1942.
- Bigg, G. R., M. R. Wadley, D. P. Stevens, and J. A. Johnson, 1996: Prediction of iceberg trajectories for the North Atlantic and Arctic Oceans. *Geophys. Res. Lett.*, **23**, 3587–3590.
- Box, J. E., D. H. Bromwich, and L. Bai, 2004: Greenland ice sheet surface mass balance 1991–2000: Application of Polar MM5 mesoscale model and in situ data. *J. Geophys. Res.*, **109**, D16105, doi:10.1029/2003JD004451.
- Church, J. A., and Coauthors, 2001: Changes in sea level. *Climate Change 2001: The Scientific Basis*, J. T. Houghton et al., Eds., Cambridge University Press, 639–693.
- Cook, K. H., 1992: The stationary response to large-scale orography in a general circulation model and a linear model. *J. Atmos. Sci.*, **49**, 525–539.
- Cox, P. M., R. A. Betts, C. B. Bunton, R. L. H. Essery, P. R. Rowntree, and J. Smith, 1999: The impact of new land surface physics on the GCM simulation of climate and climate sensitivity. *Climate Dyn.*, **15**, 183–203.
- Crowley, T. J., and S. K. Baum, 1995: Is the Greenland ice-sheet bistable? *Paleoceanography*, **10**, 357–363.
- Cubasch, U., and Coauthors, 2001: Projections of future climate change. *Climate Change 2001: The Scientific Basis*, J. T. Houghton et al., Eds., Cambridge University Press, 525–582.
- Cuffey, K. M., and S. J. Marshall, 2000: Substantial contribution to sea-level rise during the last interglacial from the Greenland ice sheet. *Nature*, **404**, 591–594.
- Drewry, D. J., and E. M. Morris, 1992: The response of large ice sheets to climatic-change. *Philos. Trans. Roy. Soc. London*, **338B**, 235–242.
- Fichefet, T., C. Poncin, H. Goosse, P. Huybrechts, I. Janssens, and H. Le Treut, 2003: Implications of changes in freshwater flux from the Greenland ice sheet for the climate of the 21st century. *Geophys. Res. Lett.*, **30**, 1911, doi:10.1029/2003GL017826.
- Gordon, C., C. Cooper, C. A. Senior, H. Banks, J. M. Gregory, T. C. Johns, J. F. B. Mitchell, and R. A. Wood, 2000: The simulation of SST, sea ice extents and ocean heat transports in a version of the Hadley Centre coupled model without flux adjustments. *Climate Dyn.*, **16**, 147–168.
- Gregory, J. M., and Coauthors, 2004: A new method for diagnosing radiative forcing and climate sensitivity. *Geophys. Res. Lett.*, **31**, L03205, doi:10.1029/2003GL018747.
- Greve, R., 2000: On the response of the Greenland ice sheet to greenhouse climate change. *Climate Change*, **46**, 289–303.
- Hanna, E., P. Huybrechts, and T. L. Mote, 2002: Surface mass balance of the Greenland ice sheet from climate-analysis data and accumulation/runoff models. *Ann. Glaciol.*, **35**, 67–72.
- Holland, M. M., and C. M. Bitz, 2003: Polar amplification of climate change in coupled models. *Climate Dyn.*, **21**, 221–232.
- Huybrechts, P., 2002: Sea-level changes at the LGM from ice-dynamic reconstructions of the Greenland and Antarctic ice sheets during the glacial cycles. *Quat. Sci. Rev.*, **21**, 203–231.
- , and J. de Wolde, 1999: The dynamic response of the Greenland and Antarctic ice sheets to multiple-century climatic warming. *J. Climate*, **12**, 2169–2188.
- , I. Janssens, C. Poncin, and T. Fichefet, 2002: The response of the Greenland ice sheet to climate changes in the 21st century by interactive coupling of an AOGCM with a thermo-mechanical ice-sheet model. *Ann. Glaciol.*, **35**, 409–415.
- Janssens, I., and P. Huybrechts, 2000: The treatment of meltwater retention in mass-balance parameterizations of the Greenland ice sheet. *Ann. Glaciol.*, **31**, 133–140.
- Kiilsholm, S., J. H. Christensen, K. Dethloff, and A. Rinke, 2003: Net accumulation of the Greenland ice sheet: High resolution modelling of climate changes. *Geophys. Res. Lett.*, **30**, 1485, doi:10.1029/2002GL015742.
- Krabbill, W., and Coauthors, 2000: Greenland ice sheet: High-elevation balance and peripheral thinning. *Science*, **289**, 428–430.
- Lefebvre, F., H. Gallee, J. P. van Ypersele, and P. Huybrechts, 2002: Modelling of large-scale melt parameters with a regional climate model in south Greenland during the 1991 melt season. *Ann. Glaciol.*, **35**, 391–397.
- Letreguilly, A., N. Reeh, and P. Huybrechts, 1991: The Greenland ice sheet through the last glacial-interglacial cycle. *Global Planet. Change*, **4**, 385–394.
- Loutre, M. F., 1995: Greenland ice sheet over the next 5000 years. *Geophys. Res. Lett.*, **22**, 783–786.
- Lunt, D. J., N. de Noblet-Ducoudre, and S. Charbit, 2004: Effects of a melted Greenland ice sheet on climate, vegetation, and the cryosphere. *Climate Dyn.*, **23**, 679–694.
- Mote, T. L., 2003: Estimation of runoff rates, mass balance, and elevation changes on the Greenland ice sheet from passive microwave observations. *J. Geophys. Res.*, **108**, 4056, doi:10.1029/2001JD002032.
- Murphy, B. F., I. Marsiat, and P. Valdes, 2002: Atmospheric contributions to the surface mass balance of Greenland in the HadAM3 atmospheric model. *J. Geophys. Res.*, **107**, 4556, doi:10.1029/2001JD000389.
- Pardaens, A. K., H. T. Banks, J. M. Gregory, and P. Rowntree, 2003: Freshwater transports in HadCM3. *Climate Dyn.*, **21**, 177–195.
- Paterson, W. S. B., and N. Reeh, 2001: Thinning of the ice sheet in northwest Greenland over the past forty years. *Nature*, **414**, 60–62.
- Payne, A. J., and Coauthors, 2000: Results from the EISMINT model intercomparison: The effects of thermomechanical coupling. *J. Glaciol.*, **46**, 227–238.
- Pope, V. D., M. L. Gallani, P. R. Rowntree, and R. A. Stratton, 2000: The impact of new physical parameterisations in the Hadley Centre climate model—HadAM3. *Climate Dyn.*, **16**, 123–146.
- Rahmstorf, S., 1995: Bifurcations of the Atlantic thermohaline circulation in response to changes in the hydrological cycle. *Nature*, **278**, 145–149.
- Rind, D., P. de Menocal, G. Russell, S. Sheth, D. Collins, G. Schmidt, and J. Teller, 2001: Effects of glacial meltwater in the GISS coupled atmosphere ocean model: North Atlantic Deep Water response. *J. Geophys. Res.*, **106**, 27 335–27 353.
- Schwierz, C., and H. C. Davies, 2002: Cyclone tracks in the vicinity of Greenland—Aspects of an interaction process. Preprints, *10th Conf. on Mountain Meteorology*, Park City, UT, Amer. Meteor. Soc., CD-ROM, 5.2.
- Steffen, K., and J. Box, 2001: Surface climatology of the Greenland ice sheet: Greenland climate network 1995–1999. *J. Geophys. Res.*, **106**, 33 951–33 964.
- Stommel, H., 1961: Thermohaline convection with two stable regimes of flow. *Tellus*, **13**, 225–230.

- Thomas, R., B. Csatho, C. Davis, C. Kim, W. Krabill, S. Manizade, J. McConnell, and J. Sonntag, 2001: Mass balance of higher-elevation parts of the Greenland ice sheet. *J. Geophys. Res.*, **106**, 33 707–33 716.
- Thorpe, R. B., J. M. Gregory, T. C. Johns, R. A. Wood, and J. F. B. Mitchell, 2001: Mechanisms determining the Atlantic thermohaline circulation response to greenhouse gas forcing in a non-flux-adjusted coupled climate model. *J. Climate*, **14**, 3102–3116.
- Toniazzo, T., J. M. Gregory, and P. Huybrechts, 2004: Climate impact of a Greenland deglaciation and its possible irreversibility. *J. Climate*, **17**, 21–33.
- Weaver, A. J., M. Eby, A. F. Fanning, and E. C. Wiebe, 1998: Simulated influence of carbon dioxide, orbital forcing and ice sheets on the climate of the Last Glacial Maximum. *Nature*, **394**, 847–853.
- Wild, M., P. Calanca, S. C. Scherrer, and A. Ohmura, 2003: Effects of polar ice sheets on global sea level in high-resolution greenhouse scenarios. *J. Geophys. Res.*, **108**, 4165, doi:10.1029/2002JD002451.
- Yoshimori, M., A. J. Weaver, S. J. Marshall, and G. K. C. Clarke, 2001: Glacial termination: Sensitivity to orbital and CO₂ forcing in a coupled climate system model. *Climate Dyn.*, **17**, 571–588.